Materials and Design 32 (2011) 255–263

Contents lists available at ScienceDirect

Materials and Design

journal homepage: www.elsevier.com/locate/matdes

Study of the characteristics of duplex stainless steel activated tungsten inert gas welds

Tsann-Shyi Chern [a], Kuang-Hung Tseng [b,*], Hsien-Lung Tsai [a]

[a] Department of Mechanical Engineering, National Taiwan University of Science and Technology, Taipei 106, Taiwan
[b] Department of Materials Engineering, National Pingtung University of Science and Technology, Pingtung 912, Taiwan

ARTICLE INFO

Article history:
Received 6 April 2010
Accepted 31 May 2010
Available online 4 June 2010

Keywords:
A. Ferrous metals and alloys
D. Welding
G. Metallography

ABSTRACT

The purpose of this study is to investigate the effects of the specific fluxes used in the tungsten inert gas (TIG) process on surface appearance, weld morphology, angular distortion, mechanical properties, and microstructures when welding 6 mm thick duplex stainless steel. This study applies a novel variant of the autogenous TIG welding, using oxide powders (TiO_2, MnO_2, SiO_2, MoO_3, and Cr_2O_3), to grade 2205 stainless steel through a thin layer of the flux to produce a bead-on-plate joint. Experimental results indicate that using SiO_2, MoO_3, and Cr_2O_3 fluxes leads to a significant increase in the penetration capability of TIG welds. The activated TIG process can increase the joint penetration and the weld depth-to-width ratio, and tends to reduce the angular distortion of grade 2205 stainless steel weldment. The welded joint also exhibited greater mechanical strength. These results suggest that the plasma column and the anode root are a mechanism for determining the morphology of activated TIG welds.

1. Introduction

Duplex stainless steel typically comprises microstructures consisting of approximately equal proportions of body-centered cubic ferrite and face-centered cubic austenite. These two phases possess varying affinities for alloying elements in duplex stainless steels [1–3]. Austenite stabilizers, such as nickel and nitrogen, concentrate in the austenite structure, while ferrite stabilizers, such as chromium and molybdenum, concentrate in the ferrite structure. Duplex stainless steel offers greater mechanical strength and higher corrosion resistance to chloride-induced stress corrosion cracking than most types of stainless steel [4–6]. Duplex stainless steel is a common structural material in the oil and gas industries, and has special applications in chemical, wastewater, and marine engineering fields as well.

The fabrication of metal structures requires the extensive use of various metal welding processes, and welding technology is an important part of materials development. TIG welding uses a non-consumable tungsten electrode that creates an arc between the electrode and the workpiece. This process is one of the most popular technologies for welding thin materials in manufacturing industries because it produces high quality welds. However, compared with the metal inert gas welding, the TIG welding has poor joint penetration when welding thick materials in a single pass [7–9]. Generally, the single pass TIG welding with argon as shielding gas is limited to a 3 mm depth for the butt-joint of stainless steels [10,11]. If the weld current increases or the travel speed decreases, the weld bead becomes excessively wide with relatively little gain in the penetration capability.

Therefore, it is necessary to improve the penetration capability and manufacturing productivity of TIG welding. One of the most notable techniques is to use activating flux with TIG welding [7–18]. To make an activating flux, powder ingredients such oxides, chlorides, and fluorides, are typically added to a solvent of acetone or ethanol. The Paton Welding Institute of Kiev (Ukraine) was the first to develop this process [19], called the activated TIG welding. Activated TIG welding improves upon conventional TIG welding, increasing the single pass joining thickness from 6 to 10 mm for stainless steel [7,12]. Using the activated TIG welding process typically results in a 200–300% increase in penetration capability [17,20], thereby reducing weld time, reducing costs for manufacturers, and avoiding cast-to-cast variations in base material compositions when using a certain flux.

The activating flux may have two types of mechanisms: one involving the Marangoni convection effect, and the other involving arc plasma behavior. The current theory on the effect of the activating flux on Marangoni convection is that active surface elements such as oxygen or sulfur in the molten pool change the fluid flow patterns by altering the surface tension gradient, resulting in a deep penetration [21–24]. However, there is little research on the action of arc plasma [25–27], and the mechanisms sustaining this effect remain unclear. Such data are very important for determining the flux ability to actually improve the joint

* Corresponding author. Tel.: +886 8 7703202; fax: +886 8 7740552.
E-mail address: tkh@mail.npust.edu.tw (K.-H. Tseng).

0261-3069/$ - see front matter © 2010 Elsevier Ltd. All rights reserved.
doi:10.1016/j.matdes.2010.05.056

penetration of TIG welds. A major concern for duplex stainless steel is that TIG welding can degrade the strength and corrosion resistance of the microstructures by producing unbalanced ferrite/austenite content in the weld metal. The phase balance of the weld metal is critical to maintaining the original chemical and physical properties of duplex stainless steel. Therefore, techniques that control the ferrite/austenite content of the weld metal are very important. This study uses five different kinds of oxide fluxes to systematically investigate the effects of single component flux on the appearance, morphology, and distortion of grade 2205 stainless steel welds. This paper studies the mechanical properties and microstructure of the weld metal and discusses the potential flux and arc interactions.

2. Experimental procedure

Grade 2205 stainless steel plate was selected as the test specimen. Table 1 lists the chemical compositions and mechanical properties of this steel. Plates measuring 6 mm thick were cut into 150 × 130 mm strips, roughly polished with 400 grit silicon carbide paper to remove surface contamination, and then cleaned with acetone. Activating flux was prepared using five kinds of single component oxides (TiO_2, MnO_2, SiO_2, MoO_3, and Cr_2O_3) packed in powdered form with about 30–60 μm particle size. These powders were mixed with acetone to produce a paint-like consistency. Before welding, a thin layer of the flux was brushed onto the surface of the joint to be welded. The coating density of flux was about 5–6 mg/cm^2. Fig. 1 shows a schematic diagram of activated TIG welding.

The autogenous TIG process was performed on the test specimen using an automatic welding machine to produce a bead-on-plate joint. A machine-mounted torch with a standard 2% thoriated tungsten electrode was used. The tip angle of the electrode was ground and the electrode gap was measured for each weld before welding to ensure that the weld was performed under the same conditions. Table 2 lists the standard welding conditions used in this study. During welding, a charge coupled device (CCD) detector was used to observe and record images of the molten pool and weld arc. To record the experimental conditions, a digital video recorder system continuously monitored the arc voltage data.

After welding, experiments were carried out to measure the angular distortion in a bead-on-plate welded joint. The mean vertical displacement method measured the distortion, as Fig. 2a schematically illustrates. A hole was drilled at the back of points P_1, P_2, and P_3, and a pillar was inserted in each hole. Three pillars (one fixed, two adjustable) were used to adjust the horizontal level, and the distance from each point to the horizontal surface was then recorded. Measurements were taken before and after welding. The differences in measurements before and after welding revealed the vertical displacement caused by welding, and the angular distortion value U can be determined as

$$|U| = \frac{(A+B)-(C+D)}{2} \quad (1)$$

where, A, B, C, and D represent the mean vertical displacement values of each point, as Fig. 2b shows.

A ferritoscope determined the ferrite content in the weld metal and base material. This device detects phases such as ferrite by their magnetic susceptibility, which differs from that of the paramagnetic austenite. To minimize measurement errors due to weld metal inhomogeneity, the average value of seven measure-

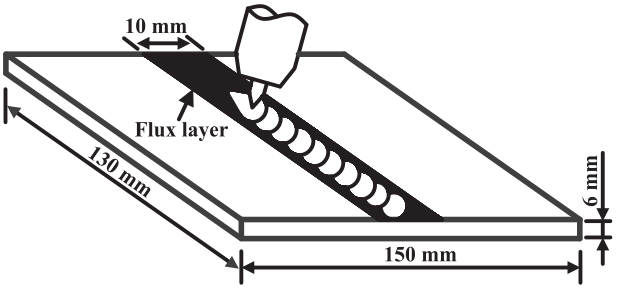

Fig. 1. Schematic diagram of activated TIG welding.

Table 2
Welding parameters for autogenous TIG welding experiments.

Weld current	200 A
Travel speed	150 mm/min
Diameter of electrode	3.2 mm
Tip angle of electrode	45°
Electrode gap	2 mm
Shielding gas	Pure argon
Gas flowrate	10 l/min

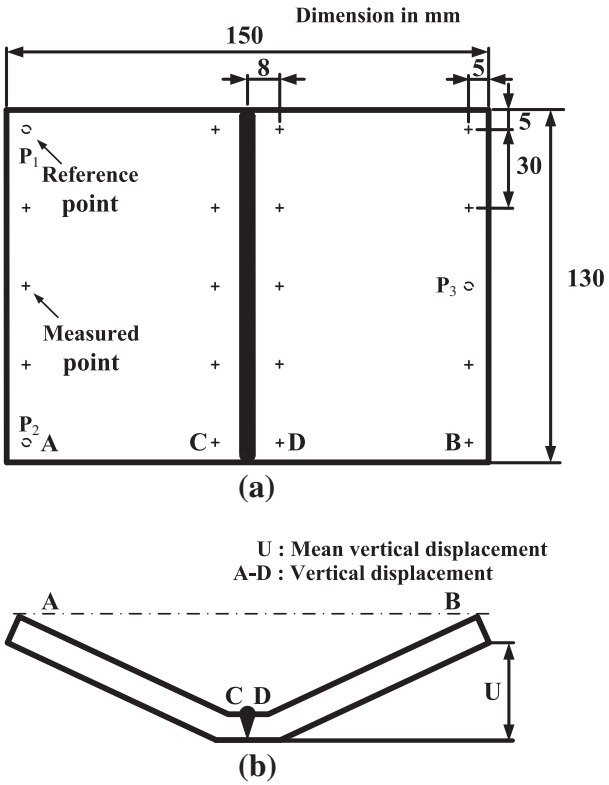

Fig. 2. Schematic diagram of distortion measurement.

Table 1
Nominal chemical composition (wt.%, balance Fe) and mechanical properties of experimental duplex stainless steels.

C	Si	Mn	P	S	Cr	Ni	Mo	N	Tensile strength, MPa	Elongation, %
0.024	0.45	0.70	0.025	0.003	21.65	5.89	3.09	0.17	765	35

ments from different locations along the welded surface was recorded.

The transverse tensile test was used to determine the metallurgical properties of the grade 2205 stainless steel weldment. The tensile tests of three specimens from each welding procedure combination were used to determine the strength and ductility of the weldment. The configuration and size of the tensile specimens were in accordance with ASTM E8. The tensile fracture mode of the weldment was also analyzed with scanning electron microscopy.

An optical microscope was used to measure the weld depth and bead width. All metallographic specimens were prepared using standard procedures, including mechanical lapping, grinding, and polishing to a 0.05 μm finish, followed by etching with a modified reagent of Kalling's solution.

3. Results and discussion

3.1. Effects of activated TIG welding on surface appearance

Fig. 3 depicts the surface appearance of grade 2205 stainless steel TIG welds with and without flux under standard welding conditions. Fig. 3a shows the results of TIG welding without flux, which produced a smooth and clean surface. Fig. 3b shows that the use of TiO_2 flux produced excessive residual slag. Fig. 3c shows that the use of MnO_2 flux created excessive residual slag and small spatters. Fig. 3d shows a satisfactory surface appearance for the grade 2205 stainless steel welds obtained using SiO_2 flux. Fig. 3e shows that MoO_3 flux produced litter residual slag and large spatters. Fig. 3f shows that Cr_2O_3 flux produced excessive residual slag and large spatters. These experimental results clearly indicate that the TIG welded surface produced with oxide fluxes contributed to the formation of residual slag and spatters. Moreover, the activated TIG welding process produces a small amount of fume.

3.2. Effects of activated TIG welding on weld morphology

Fig. 4 shows the cross-sections of the TIG welds in 6 mm thick grade 2205 stainless steels with and without flux. The TIG welds exhibit a significant variation in weld depth and bead width; TIG welds without flux exhibited a wide and shallow morphology (Fig. 4a), while the TIG welds with oxide flux exhibited a narrow and deep morphology (Fig. 4b–f). This study shows that the greatest improvement in TIG penetration capability occurred with the use of SiO_2 flux. This flux achieved a 295% improvement compared with the conventional TIG process. Fig. 4 shows that TIG welding with flux can significantly increase the weld depth-to-width ratio. According to investigations by Tseng and Chou [28,29], a deep joint weld with a high depth-to-width ratio is characteristic of the increased the input energy density of the heat source, which produces a high degree of heat energy concentration during activated TIG welding. The SiO_2 flux can facilitate full joint penetration and achieve a satisfactory surface appearance for grade 2205 stainless steel activated TIG welds.

3.3. Mechanism for increased activated TIG penetration capability

Heiple and Roper proposed that the direction of fluid flow in a molten pool can affect the weld morphology, and that surface tension gradient is the major factor driving fluid flow [21–23]. In TIG

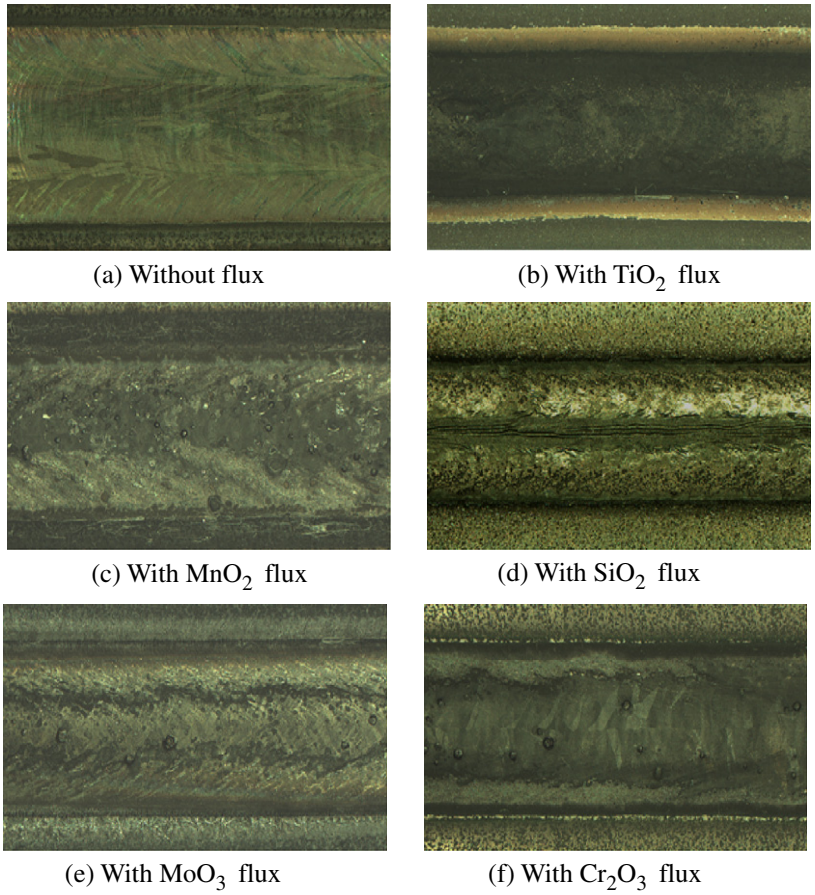

Fig. 3. Effect of oxide flux on surface appearance.

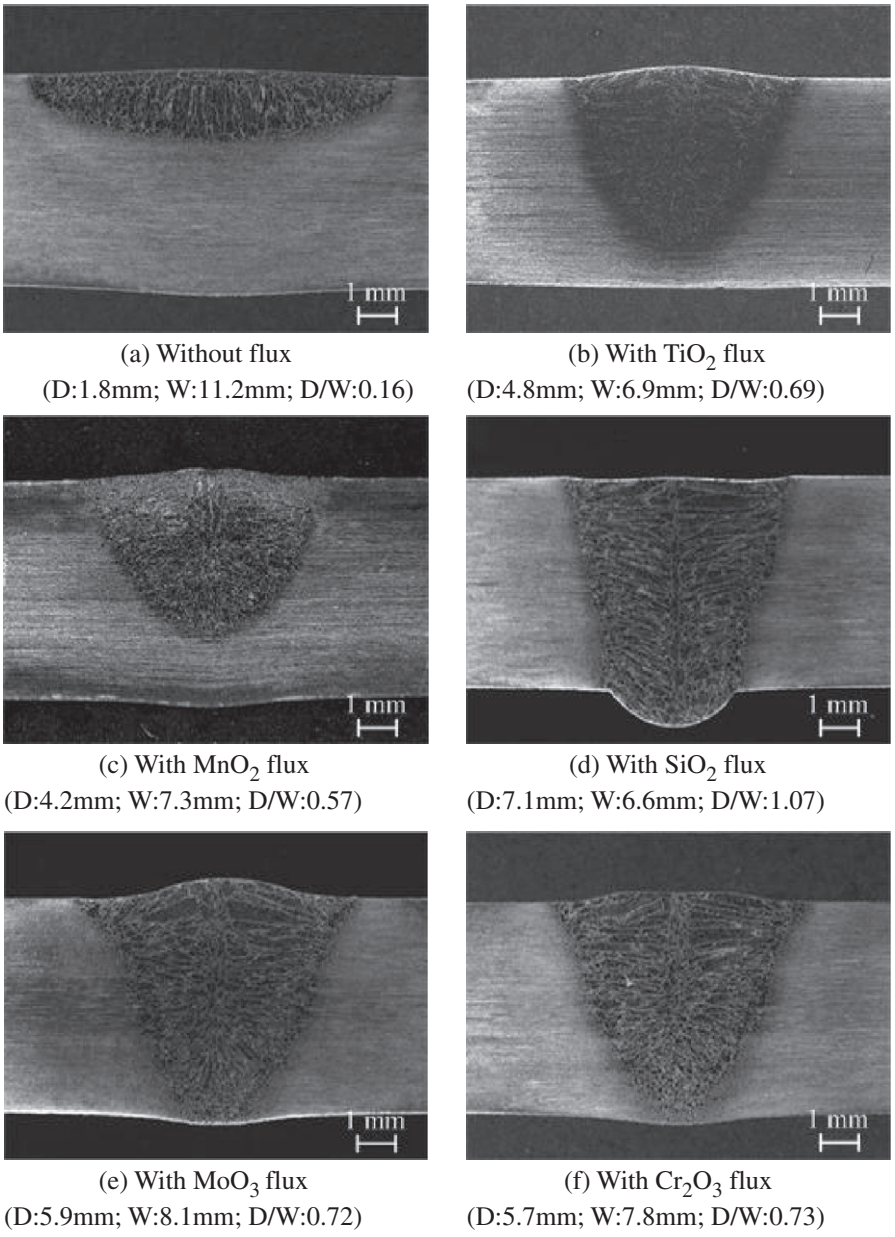

(a) Without flux (D:1.8mm; W:11.2mm; D/W:0.16)

(b) With TiO_2 flux (D:4.8mm; W:6.9mm; D/W:0.69)

(c) With MnO_2 flux (D:4.2mm; W:7.3mm; D/W:0.57)

(d) With SiO_2 flux (D:7.1mm; W:6.6mm; D/W:1.07)

(e) With MoO_3 flux (D:5.9mm; W:8.1mm; D/W:0.72)

(f) With Cr_2O_3 flux (D:5.7mm; W:7.8mm; D/W:0.73)

Fig. 4. Effect of oxide flux on weld morphology.

molten pools, there is always a temperature gradient on the molten pool surface, with high temperatures in the pool center under the arc and low temperatures at the pool edge. For TIG welding without flux, the surface tension decreases as the temperature increases. In this condition, the surface tension is highest at the edge of the pool and lowest at the center of the pool. This surface tension gradient $d\sigma/dT$ produces an outward surface fluid flow, as Fig. 5a indicates, and generates a wide and shallow weld geometry, as Fig. 4a shows. For TIG welding with oxide fluxes, adding surface active element oxygen to the molten pool can drastically change the temperature dependence of surface tension. In this condition, the surface tension will be highest at the pool center, creating an inward surface fluid flow result, as Fig. 5b illustrates. Fig. 4b–f shows that this surface fluid flow pattern produces a narrow and deep weld geometry.

Fig. 4 also shows that the increase in the weld depth-to-width ratio with oxide fluxes was either weak or strong, depending on the chemical composition of the flux. The SiO_2, MoO_3, and Cr_2O_3 fluxes produced relatively deep TIG penetration, while the TiO_2 and MnO_2 fluxes produced relatively shallow TIG penetration. At present, there is no consensus on the mechanism through which the activating flux increases TIG joint penetration. Heiple et al. suggested that the inward fluid flow is a major mechanism for increasing the joint penetration of activated TIG welds [21–24]. However, they did not account for the potential interactions between the flux and arc. Arc constriction may play a major role in determining the joint penetration. Although its exact mechanism remains unclear, researchers have used arc constriction to create TIG welds with a deep joint penetration [25–27].

An arc consists of a sustained electrical discharge through a high temperature conducting plasma that produces heat energy. Fig. 6 indicates that a direct-current TIG arc consists of three regions, according to its voltage distribution. These regions are the cathode space (the region adjacent to the electrode), anode space (the region adjacent to the base material), and plasma column (the central region). The cooling effects of the electrode and base

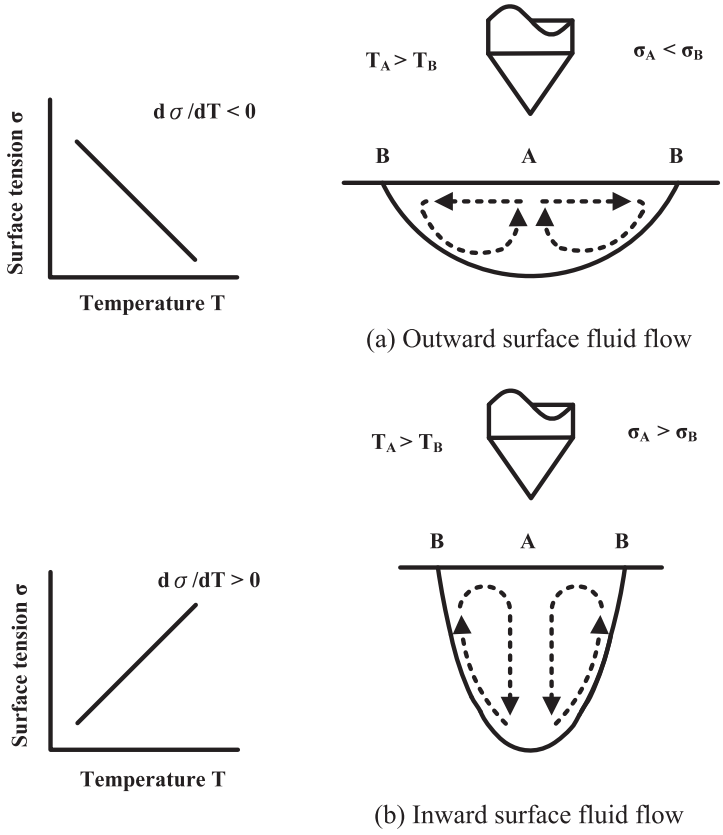

Fig. 5. Schematic diagram of surface fluid flow pattern.

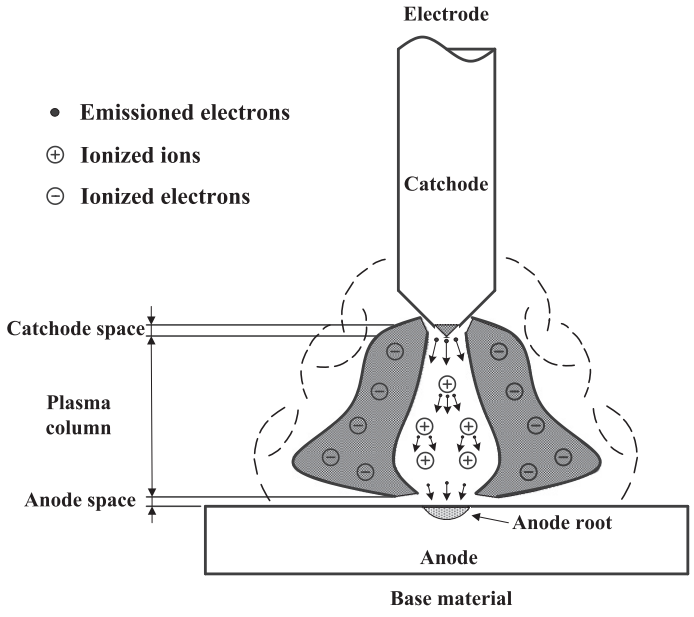

Fig. 6. Schematic diagram of the direct-current TIG arc.

material cause a rapid drop in voltage at the end regions. In plasma column, a circular magnetic field surrounds the arc, and the thermal ionization of the gas produces a current carried by the ions and electrons. The electrons are the major charge carriers.

The role of an arc during TIG welding with and without flux was investigated using a CCD detector. The arc images in Fig. 7 provides a clear experimental verification of the effect of the fluxes on an arc. The activated TIG arc constricts the diameter of the plasma column and reduces the area of the anode root compared with the conventional TIG arc at the same current level. In the central region of the TIG arc, the arc plasma temperature is higher than the dissociation temperature of the ionic flux and shielding gas, and the ionized atoms and molecules generate positive ions and electrons. In the peripheral regions of the plasma column, however, the dis-

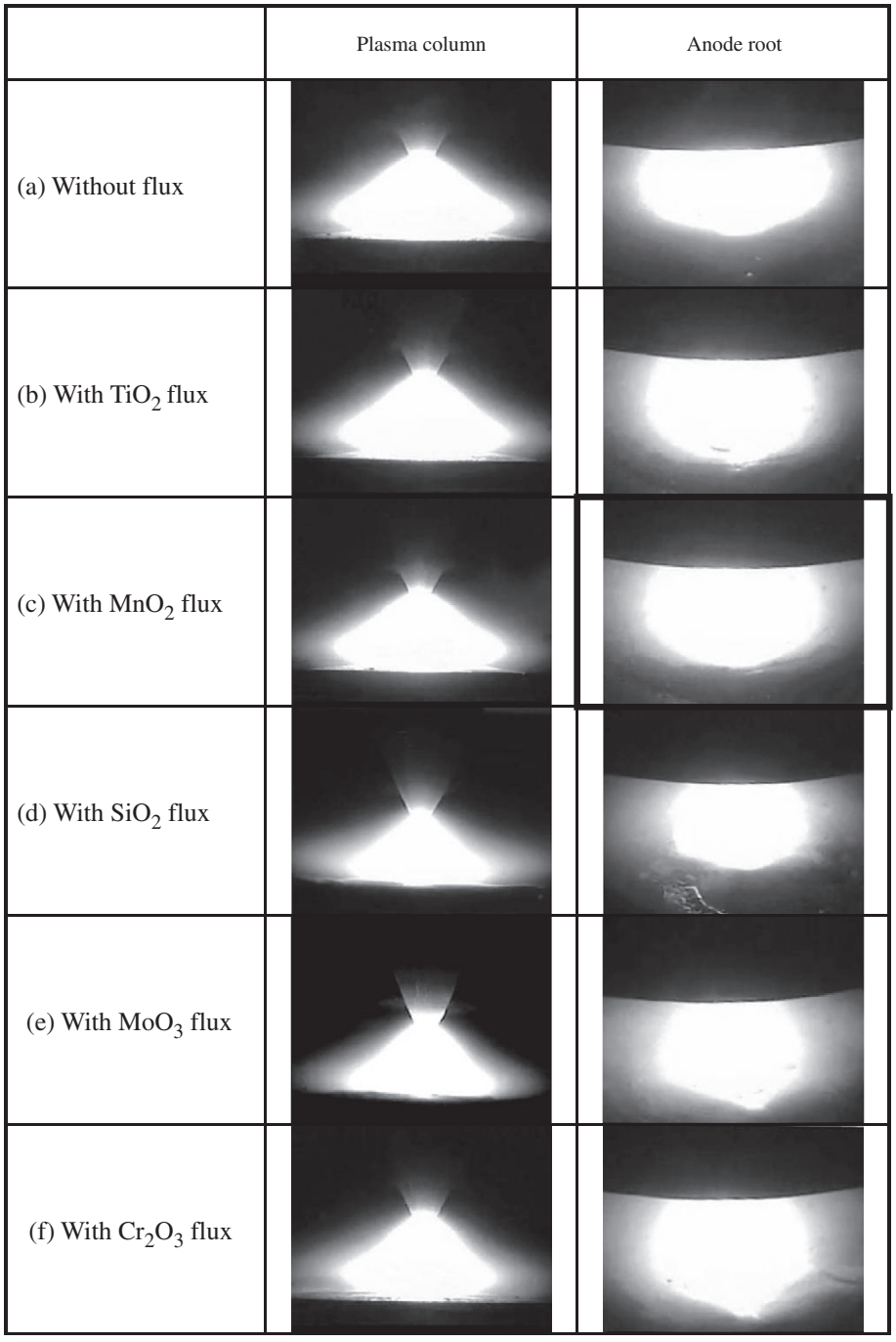

Fig. 7. Effect of oxide flux on plasma column and anode root.

solved flux still exists as atoms or molecules large enough for the electrons to attach and form the negative charges. The process of electron attachment occurs only in the peripheral region of the plasma column, where there is a weak electric field and arc temperature is lower. Consequently, a reduction in the number of electrons in the peripheral plasma region, which are major charge carriers, constricts the diameter of the plasma column. At the same time, the area of the anode root also decreases. Fig. 7 shows that the anode root is clearly visible. Constriction of the plasma column increases the energy density in the anode root, achieving a more focused arc in the penetration capability of activated TIG welds compared with conventional TIG welds. These results suggest that the plasma column and the anode root is a mechanism that determines TIG penetration capability with use of the certain fluxes. Physically constricting the plasma column and reducing the anode root not only increased the weld depth, but also decreased the bead width when using the activated TIG process.

The fact that flux composition determines the degree of plasma column constriction is a notable finding. When using SiO_2, MoO_3, and Cr_2O_3 fluxes in TIG welding, the heat of the arc plasma melts and ionizes a part of the oxide flux. Fig. 7d–f shows that the interaction of oxygen ions with arc electrons redistributes the charger carriers, and constricts the plasma column by capturing electrons in the outer regions of weld arc. This effect can create a significant increase in energy density and arc temperature acting on the anode root. In turn, an increased electromagnetic force (Lorentz force) can lead to a strong downward flow in the liquid metal along the pool center. This creates a significant increase in the weld depth-to-

width ratio (Fig. 4d–f) compared with the TIG welding with the use of TiO_2 and MnO_2 fluxes (Fig. 4b and c). Future research should investigate the physical mechanisms involved in this process. These findings may support the present study, which potentially demonstrates the effect of specific fluxes on activated TIG penetration capability.

Fig. 8 shows the effect of TIG welding on arc voltage with and without flux. The weld current and travel speed were maintained at a constant value, and the arc voltage increased when the activated TIG welding was used. As the energy density of the activated TIG weld arc increases, the arc voltage must also increase to develop the proper current continuity with the arc plasma, which is at a higher temperature and has greater energy density. In addition, the arc contains many free electrons. The decomposed flux additives attract electrons, causing the arc to constrict and result in an increase in arc voltage. Fig. 8 clearly shows that the five fluxes can simultaneously increase the arc voltage, whereas the increase caused by the oxides can be weak or strong depending on the flux compositions. There is a clear correlation between the measured arc voltage and the observed arc constriction in TIG welding with and without flux, i.e., the higher the arc voltage value, the greater weld arc constriction will be.

3.4. Effects of activated TIG welding on angular distortion

During welding, a joint plate is locally heated by the arc, and the temperature distributions in the weldment are not uniform. Heating and cooling cycles induce non-uniform thermal strains in both the weld metal and the adjacent base metal, and plastic upsetting accompanies the thermal strains produced during heating. The non-uniform thermal stresses resulting from these strains combine and react to produce internal forces that cause shrinkage and distortion. Angular distortion often occurs in a welded plate when transverse shrinkage is not uniform in the thickness direction. Fig. 9 shows the effects of TIG welding on the angular distortion of the grade 2205 stainless steel weldment with and without flux. Activated TIG welding increases both the joint penetration and the weld depth-to-width ratio. This is characteristic of a high degree of energy concentration during welding, and reduces the quantity of supplied heat. This in turn prevents overheating of the base material, and reduces the incidence of thermal strains and incompatible strain caused by shrinkage in thickness. Therefore, this approach reduces the angular distortion of the grade 2205 stainless steel activated TIG weldment. Note that the variations in angular distortion values are associated with a weld depth relative to plate thickness and the shape and dimensions of welds [28,30,31]. Therefore, a full joint penetration and the greatest weld depth-to-width ratio resulted in the lowest angular distortion. A reduction of shrinkage and distortion is critical to improving the weld quality of finished structures. In this study, the grade 2205 stainless steel TIG welding with SiO_2 flux produced a significant increase in the joint penetration and the weld depth-to-width ratio were about 7.1 mm and 1.07, respectively. Consequently, the angular distortion of the weldment value was almost zero.

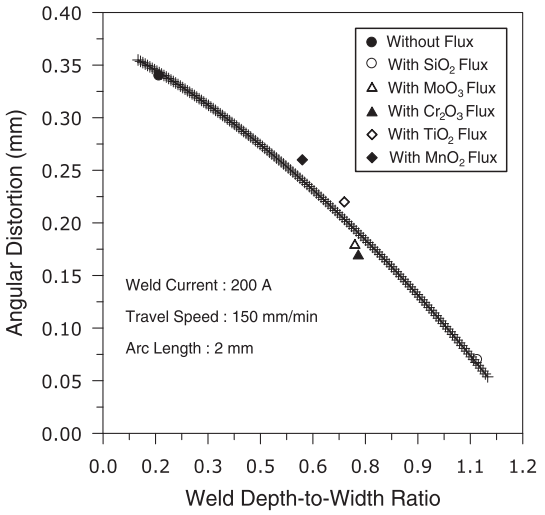

Fig. 9. Effect of oxide flux on angular distortion.

3.5. Effects of activated TIG welding on ferrite and austenite content

The experiments in this study used grade 2205 hot rolled stainless steel plate as the base material. The microstructures of this material consisted of 54.1% austenite and 45.9% ferrite. Fig. 10 presents the measured content of ferrite and austenite in the duplex stainless steel TIG weld metal produced with and without flux. In the grade 2205 stainless steel TIG weld metal produced without flux, the measured ferrite content increased from its initial value of 45.9–63.4%. This is because the weld metal of duplex stainless steel solidifies primarily as delta ferrite. During welding, weld metal cools so rapidly that the transformation of delta ferrite to aus-

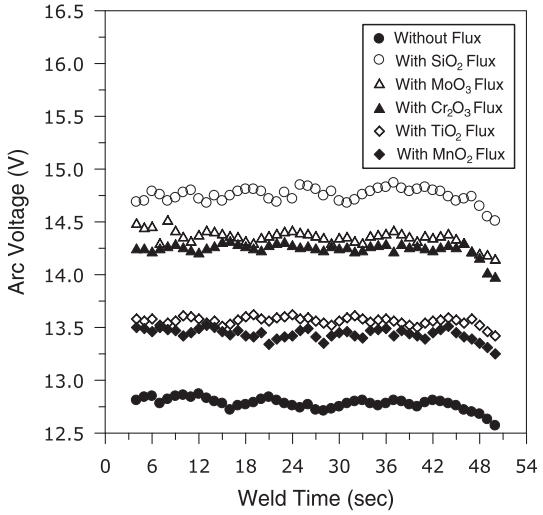

Fig. 8. Effect of oxide flux on arc voltage.

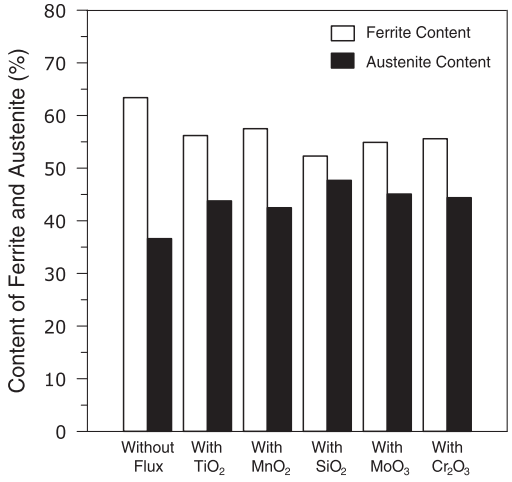

Fig. 10. Effect of oxide flux on content of ferrite and austenite.

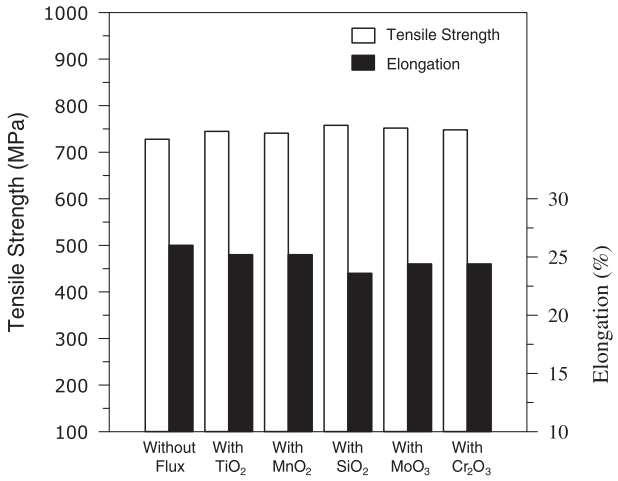

Fig. 11. Effect of oxide flux on mechanical properties.

tenite is not complete, and consequently, more ferrite forms in the TIG weld metal after solidification. Using oxide fluxes increased the measured ferrite content in activated TIG weld metal to 52.3–57.5%. The ferrite content of the grade 2205 stainless steel TIG weld metal produced with flux was lower than that of the weld metal without flux. This result is due to the weld heat input. Heat input is a relative measure of the heat energy transferred per unit length of weld. Since the calculated heat input is proportional to the measured arc voltage, the applied flux increases the heat input. Therefore, there is an increase in the peak temperature of the weld metal and a reduction in the cooling rate. In this case, the transformation of delta ferrite to austenite is complete or ceases to attain the equilibrium phases, resulting in a lower ferrite content in grade 2205 stainless steel activated TIG weld metal. In this study, the grade 2205 stainless steel TIG weld metal produced using SiO_2 flux possessed microstructures consisting of approximately equal proportions of ferrite (52.3%) and austenite (47.7%) at room temperature.

3.6. Effects of activated TIG welding on mechanical properties

The grade 2205 duplex stainless steel base material used in this study has a tensile strength and elongation of 765 MPa and 35%, respectively. Fig. 11 presents the experimental results for the mechanical properties of TIG weldment with and without flux. The base material used in this present study is wrought alloys, which have better mechanical properties than as-welded alloys because of work hardening. Fig. 11 shows that the grade 2205 stainless steel joints obtained using TIG process with flux presented equal or better tensile strength than that of TIG weldment made without flux. However, the dependence of ductility, as a percentage of elongation, shows a slight reduction with the use of flux for grade 2205 stainless steel TIG joint. Ordinarily, strengthening an alloy decreases its ductility.

In the tensile test, all weldments failed on the weld metals. Technically, a fracture is a single body separated into pieces by imposed stress. For engineering materials, there are only two possible modes of fracture: ductile and brittle. Fig. 12 shows the secondary electron micrographs of the fracture surface of the grade 2205 stainless steel TIG weldment with and without SiO_2 flux. In all cases, the microstructures exhibited ductile fractures in the form of dimples or microvoids.

4. Conclusions

This study systematically investigates the effects of TiO_2, MnO_2, SiO_2, MoO_3, and Cr_2O_3 fluxes on surface appearance, weld morphology, angular distortion, ferrite/austenite content, and mechanical properties obtained with the TIG process applied to 6 mm thick grade 2205 stainless steels. The experimental results in this study provide the following conclusions:

1. The surface of TIG welds produced with flux formed residual slag and spatters. Using TIG welding with flux produced a small amount of fume.
2. Using SiO_2, MoO_3, and Cr_2O_3 fluxes not only significantly increased penetration capability, but also improved mechanical strength of the grade 2205 stainless steel welds compared with conventional TIG welds.
3. The plasma column and the anode root mechanisms can determine TIG penetration capability using certain fluxes. Physically constricting the plasma column and reducing the anode root increased the weld depth and decreased the bead width for the activated TIG process.
4. Using activated TIG welding increased both the joint penetration and the weld depth-to-width ratio. This in turn reduced the angular distortion of the grade 2205 stainless steel activated TIG weldment. In this study, grade 2205 stainless steel TIG welding with SiO_2 flux produced a full joint penetration and the greatest weld depth-to-width ratio. As a result, the angular distortion value was almost zero.
5. Activated TIG welding increased the arc voltage, and the amount of heat input level can therefore be increased. As a result, the ferrite content of the grade 2205 stainless steel activated TIG weld metal is decreased.

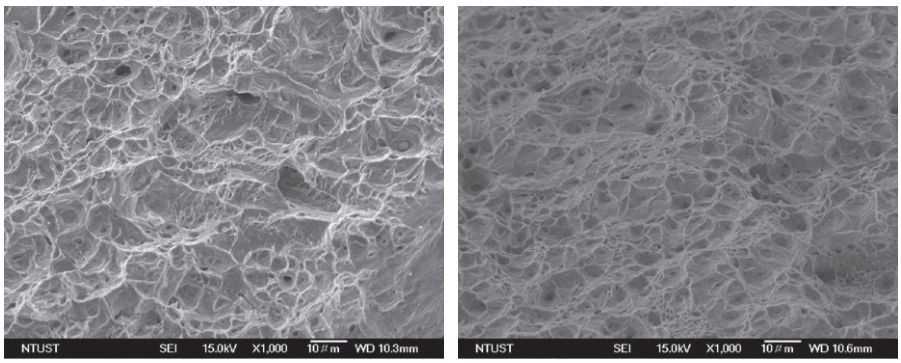

(a) Without flux (b) With SiO_2 flux

Fig. 12. Scanning electron micrograph of fracture surface.

Acknowledgment

The authors gratefully acknowledge the financial support for this research provided by the National Science Council, Taiwan, Republic of China, under Grant No. NSC 97-2218-E-020-003.

References

[1] Miura M, Koso M, Kudo T, Tsuge H. The effect of nickel and nitrogen on the microstructure and corrosion resistance of duplex stainless steel weldment. Weld Int 1990;4(3):200–6.
[2] Cortie MB, Potgieter JH. The effect of temperature and nitrogen content on the partitioning of alloy elements in duplex stainless steels. Metall Trans A 1991;22A:2173–9.
[3] Sun Z, Kuo M, Annergren I, Pan D. Effect of dual torch technique on duplex stainless steel welds. Mater Sci Eng A 2003;356:274–82.
[4] Sridhar N, Kolts J, Flashe LH. A duplex stainless steels for chloride environments. J Metals 1985;37(3):31–5.
[5] Tsai ST, Yen KP, Shih HC. The embrittlement of duplex stainless steel in sulfide-containing 3.5 wt% NaCl solution. Corros Sci 1998;40:281–95.
[6] Iris Alvarez-Armas. Duplex stainless steels: brief history and some recent alloys. Recent Pat Mech Eng 2008;1:51–7.
[7] Huang HY, Shyu SW, Tseng KH, Chou CP. Evaluation of TIG flux welding on the characteristics of stainless steel. Sci Technol Weld Join 2005;10(5):566–73.
[8] Shyu SW, Huang HY, Tseng KH, Chou CP. Study of the performance of stainless steel A-TIG welds. J Mater Eng Perform 2008;17(2):197–201.
[9] Fujii H, Sato T, Lu SP, Nogi K. Development of an advanced A-TIG (AA-TIG) welding method by control of Marangoni convection. Mater Sci Eng A 2008;495:296–303.
[10] Huang HY, Shyu SW, Tseng KH, Chou CP. Effects of the process parameters on austenitic stainless steel by TIG-flux welding. J Mater Sci Technol 2006;22(3):367–74.
[11] Lu SP, Li DZ, Fujii H, Nogi K. Time dependant weld shape in Ar–O_2 shielded stationary GTA welding. J Mater Sci Technol 2007;23(5):650–4.
[12] Leconte S, Paillard P, Chapelle P, Henrion G, Saindrenan J. Effect of oxide fluxes on activation mechanisms of tungsten inert gas process. Sci Technol Weld Join 2006;11(4):389–97.
[13] Li QM, Wang XH, Zou ZD, Wu J. Effect of activating flux on arc shape and arc voltage in tungsten inert gas welding. Trans Nonferr Metals Soc China 2007;17:486–90.
[14] Liu LM, Zhang ZD, Song G, Wang L. Mechanism and microstructure of oxide fluxes for gas tungsten arc welding of magnesium alloy. Metall Mater Trans A 2007;38A:649–58.
[15] Xu YL, Dong ZB, Wei YH, Yang CL. Marangoni convection and weld shape variation in A-TIG welding process. Theor Appl Fract Mech 2007;48:178–86.
[16] Zhang ZD, Liu LM, Shen Y, Wang L. Mechanical properties and microstructures of a magnesium alloy gas tungsten arc welded with a cadmium chloride flux. Mater Charact 2008;59:40–6.
[17] Liu L, Sun H. Study of flux assisted TIG welding of magnesium alloy with SiC particles in flux. Mater Res Innovat 2008;12(1):47–51.
[18] Huang HY. Effects of shielding gas composition and activating flux on GTAW weldments. Mater Des 2009;30:2404–9.
[19] Gurevich SM, Zamkov VN, Kushnirenko NA. Improving the penetration of titanium alloys when they are welded by argon tungsten arc process. Avtomatichesk Svar 1965;9:1–4.
[20] Marya M, Edwards GR. Chloride contributions in flux-assisted GTA welding of magnesium alloys. Weld J 2002;81(12):291s–8s.
[21] Heiple CR, Roper JR. Effect of selenium on GTAW fusion zone geometry. Weld J 1981;60(8):143s–5s.
[22] Heiple CR, Roper JR. Mechanism for minor element effect on GTA fusion zone geometry. Weld J 1982;61(4):97s–102s.
[23] Heiple CR, Roper JR, Stagner RT, Aden RJ. Surface active element effects on the shape of GTA, laser, and electron beam welds. Weld J 1983;62(3):72s–7s.
[24] Heiple CR, Burgardt P. Effect of SO_2 shielding gas addition on GTA weld shape. Weld J 1985;64(6):159s–62s.
[25] Simonik AG. The effect of contraction of the arc discharge upon the introduction of electro-negative elements. Svar Proiz 1976;3:49–51.
[26] Lucas W, Howse D. Activating flux – increasing the performance and productivity of the TIG and plasma processes. Weld Metal Fabricat 1996;64(1):11–7.
[27] Howse DS, Lucas W. Investigation into arc constriction by active fluxes for tungsten inert gas welding. Sci Technol Weld Join 2000;5(3):189–93.
[28] Tseng KH, Chou CP. Effect of pulsed gas tungsten arc welding on angular distortion in austenitic stainless steel weldments. Sci Technol Weld Join 2001;6(3):149–53.
[29] Tseng KH, Chou CP. The effect of pulsed GTA welding on the residual stress of a stainless steel weldment. J Mater Process Technol 2002;123:346–53.
[30] Pavlovsky VI, Masubuchi K. Research in the USSR on residual stresses and distortion in welded structures. Weld Res Counc Bull 1994;388:44–8.
[31] Tseng KH, Chou CP. The study of nitrogen in argon gas on the angular distortion of austenitic stainless steel weldments. J Mater Process Technol 2003;142:139–44.